scientific reports

Check for updates

OPEN

Electronic fluctuation difference between trimethylamine *N*-oxide and *tert*-butyl alcohol in water

Nahoko Kuroki[1,2✉], Yukina Uchino[3], Tamon Funakura[1] & Hirotoshi Mori[1,4✉]

Although small organic molecules in cells have been considered important to control the functions of proteins, their electronic fluctuation and the intermolecular interaction, which is physicochemical origin of the molecular functions, under physiological conditions, i.e., dilute aqueous solutions (0.18 mol L^{-1}), has never been clarified due to the lack of observation methods with both accuracy and efficiency. Herein, the time evolutions of the interactions in dilute aqueous trimethylamine *N*-oxide (TMAO) and *tert*-butyl alcohol (TBA) solutions were analyzed via ab initio molecular dynamics simulations accelerated with the fragment molecular theory. It has been known that TMAO and TBA have similar structures, but opposite physiological functions to stabilize and destabilize proteins. It was clarified that TMAO induced stable polarization and charge-transfer interactions with water molecules near the hydrophilic group, and water molecules were caught even near the CH$_3$– group. Those should affect protein stabilization. Understanding the solution dynamics will contribute to artificial chaperone design in next generation medicine.

Small organic solutes in cells have various effects on proteins. For example, trimethylamine *N*-oxide (TMAO, Fig. S1a), which consists of N$^+$O$^-$ and methyl (CH$_3$–) groups, has been found in deep-sea fishes and is a known osmolyte that preserves the physiological functions of proteins[1]. The effects are often compared with the ions like (CH$_3$)$_4$ N$^+$ and PO$_4^{3-}$ that are more capable of structuring water in the Hofmeister series[2]. However, the preservation mechanism of the osmotic pressure is still under debate; the proposed explanations include an attractive direct interaction between TMAO and proteins[2] or indirect interactions via structural changes of an aqueous solution as a molecular aggregate[3,4]. If the mechanism by which TMAO allows physiological functional preservation in proteins is clarified, it would make fundamental scientific contributions to, for example, the next generation of medicine by accelerating the development of artificial chaperones and understanding the mechanism of atherosclerosis.

The biophysical chemistry and solution dynamics of aqueous TMAO solutions have been extensively investigated from experimental[5–14] viewpoints. Vibrational and nuclear magnetic resonance spectroscopy indicated that both the N$^+$O$^-$ and CH$_3$– groups of TMAO slow the dynamics of water molecules in a solution and that the N$^+$O$^-$ groups have a notable ability to capture water molecules[5–7,10,11,13]. These results have been carefully discussed by molecular dynamics simulations based on classical force fields[3,15–18]. However, it is well known that the results depend on the choice of the force field. Thus, ab initio molecular dynamics (AIMD) simulations are essential for explaining the experimental results precisely and designing the osmotic pressure regulation ability artificially. Although there have been several sub-picosecond-order Born–Oppenheimer AIMD simulations with the density functional theory[19–24], previous studies have not revealed the intermolecular interaction, which is physicochemical origin of the molecular functions. Additionally, due to the high computational costs of the previous AIMD simulations, the target systems were limited within the small sizes, and the concentrations (over 0.5 mol L^{-1}) were much higher than natural conditions (i.e., those in deep-sea fishes).

The object of this study is to clarify the electronic fluctuation and the temporal evolution of intermolecular interactions in TMAO aqueous solution with a realistic condition of concentration. For this purpose, we focused on solute–solvent interactions and applied the ab initio effective fragment potential-molecular dynamics simulation (EFP-MD), which is particularly suited to performing nanosecond-order AIMD simulations for systems containing several thousand atoms[25–30], for dilute aqueous TMAO solutions (0.18 mol L^{-1}). For comparison, a

[1]Department of Applied Chemistry, Faculty of Science and Engineering, Chuo University, Bunkyo-ku, Tokyo 112-8551, Japan. [2]JST, ACT-X, Kawaguchi, Saitama 332-0012, Japan. [3]Department of Chemistry and Biochemistry, Graduate School of Humanities and Sciences, Ochanomizu University, Bunkyo-ku, Tokyo 112-8610, Japan. [4]Department of Theoretical and Computational Molecular Science, Institute for Molecular Science, Myodaiji, Okazaki 444-8585, Japan. ✉email: kuroki.91d@g.chuo-u.ac.jp; qc-forest.19d@g.chuo-u.ac.jp

dilute aqueous solution of *tert*-butyl alcohol (TBA, Fig. S1b), which is known as a protein denaturant[5,6,16], was also investigated.

Computational method

The structures of TMAO, TBA, and H_2O molecules in the gas phase were optimized using the Gaussian16 quantum chemistry program package[31]. The MP2/aug-cc-pVTZ[32] level of theory was applied to the calculations, and the natural bond orbital (NBO) analysis was performed. The T_1 diagnostic values[33] of TMAO, TBA, and H_2O molecules were 0.013, 0.010, and 0.010, respectively, confirming that there was no multireference nature. Using the wavefunctions for the optimized molecules, the EFPs at the aug-cc-pVTZ basis function were uniquely defined by the "MAKEFP" module implemented in the GAMESS-US program package[34].

Before performing the EFP-MD simulations, we evaluated the accuracy of the EFPs. For this purpose, we decomposed the total interaction energies obtained by the quantum chemistry calculations (MP2/aug-cc-pVTZ) into electrostatic (E^{ES}), exchange-repulsion (E^{EXREP}), polarization with charge-transfer ($E^{POL} + E^{CT}$), and dispersion (E^{DISP}) interaction energy components through localized molecular orbital energy decomposition analysis (LMO-EDA)[35] and compared them with the EFP results. In the LMO-EDA calculations, we applied the counterpoise method to correct the basis set superposition errors.

Subsequently, we performed a set of EFP-MD simulations for dilute aqueous TMAO or TBA solutions and pure water. In the EFP-MD simulations, we used a set of cubic periodic boxes with a side length of ~ 21 Å containing one solute molecule and 300 H_2O molecules with a canonical (NVT) ensemble and a cutoff distance of 10 Å. Damping expressions were applied for long-range terms[25]. The simulation box size was defined to model the dilute aqueous solution (0.18 mol L^{-1}), which was realistic concentration for deep-sea fishes. In the EFP-MD simulations, we used a time step of 1 fs and a temperature of 298.15 K (defined using a Nosé–Hoover thermostat). Under these conditions, a set of at least 0.8 ns equilibration and 2.5 ns production runs was performed to evaluate the self-diffusion constants, radial distribution functions (RDFs), and time-dependent intermolecular interaction energies.

Results and discussion

The chemical accuracy of EFPs was verified for TMAO, TBA, and H_2O. The EFPs reproduced dipole moments via high-precision ab initio quantum chemistry calculations within a 0.14 D error, which is more accurate than that of well-trained classical force field models[16,17] (Table S1). The structural parameters of TMAO/TBA–H_2O dimer models optimized by the EFPs agreed with the MP2 level of quantum chemistry calculation results within 0.14 Å (Figs. S2, S3, and Tables S2, S3). The slight difference in dimer formation validates the rigid rotor approximation in the EFP method, at least within our target systems. The total interaction energy and its components, calculated by the EFP method, near the stable conformation of the TMAO/TBA–H_2O dimer, accurately reproduced the corresponding LMO-EDA at the MP2 level (Figs. S4, S5). The mean absolute error (MAE) of the total interaction energy obtained by EFP and MP2 was 2.0 kcal mol^{-1}. The MAE of each interaction energy component (E^{ES}, E^{EXREP}, $E^{POL} + E^{CT}$, and E^{DISP}) was 1.0, 0.6, 1.9, and 0.6 kcal mol^{-1}, respectively. The H_2O–H_2O interaction described by the EFP method has been established previously[29]. The chemical accuracy of the EFP method was thus confirmed. It should be noted that there is no cumbersome fitting in the definition of EFPs.

One of the ways to discuss the transport properties by MD simulations is calculating the self-diffusion coefficients using Einstein's equation (Eq. 1).

$$D = \lim_{t \to \infty} \frac{1}{6t} \langle |\boldsymbol{r}_i(t) - \boldsymbol{r}_i(0)|^2 \rangle \tag{1}$$

The diffusion coefficient of water (D_{water}) was experimentally observed to be 2.3×10^{-9} m^2 s^{-1}[36], and it has been also reported that D_{water} in a dilute aqueous TMAO/TBA solution (~ 0.2 mol L^{-1}) is ~ 10% lower than that in pure water[6,18,37]. Our nanosecond-order ab initio EFP-MD results successfully reproduced that these solutes slow the dynamics of water molecules (Table S4).

Several solute–solvent site RDFs were calculated to investigate dilute aqueous TMAO/TBA solutions (Fig. 1 and Table S5). The coordination numbers of the top sites of solutes were evaluated by integrating the RDFs for $O_{TMAO/TBA}$–O_{water} and $O_{TMAO/TBA}$–H_{water} for the range up to the first minima. The coordination number calculated using $O_{TMAO/TBA}$–O_{water} was 3.3 for both TMAO and TBA, while those calculated using $O_{TMAO/TBA}$–H_{water} were 3.3, and 2.0 for TMAO and TBA, respectively. These results indicate that the hydrophilic groups of TMAO firmly trap three H_2O molecules as hydrogen-bond donors, while those of TBA coordinate two H_2O molecules and one H_2O molecule as hydrogen-bond donors and acceptor, respectively. Focusing on the bottom sites of TMAO and TBA, i.e., the coordination numbers of $X_{TMAO/TBA}$–O_{water}, it is apparent that the CH_3– groups of TMAO and TBA have different hydration properties. Therefore, the RDFs for X_{TBA}–O_{water} have no peaks within 2 Å, while X_{TMAO}–O_{water} has a coordination number of 0.7. The CH_3– groups of TBA exhibit "hydrophobic hydration," while those of TMAO proactively trap H_2O molecules. The CH_3– groups of TMAO and TBA enact differently in dilute solutions[5,18].

The TMAO/TBA···H_2O interaction correlation function ($p(t)$)[38] (Eq. 2) was calculated to clarify the effect of the N^+O^-, OH, and CH_3– groups of each solute on the kinetics of the water molecules in the dilute aqueous TMAO/TBA solutions (Fig. S6).

$$p(t) = \frac{\langle h(0)h(t) \rangle}{\langle h(0) \rangle} \tag{2}$$
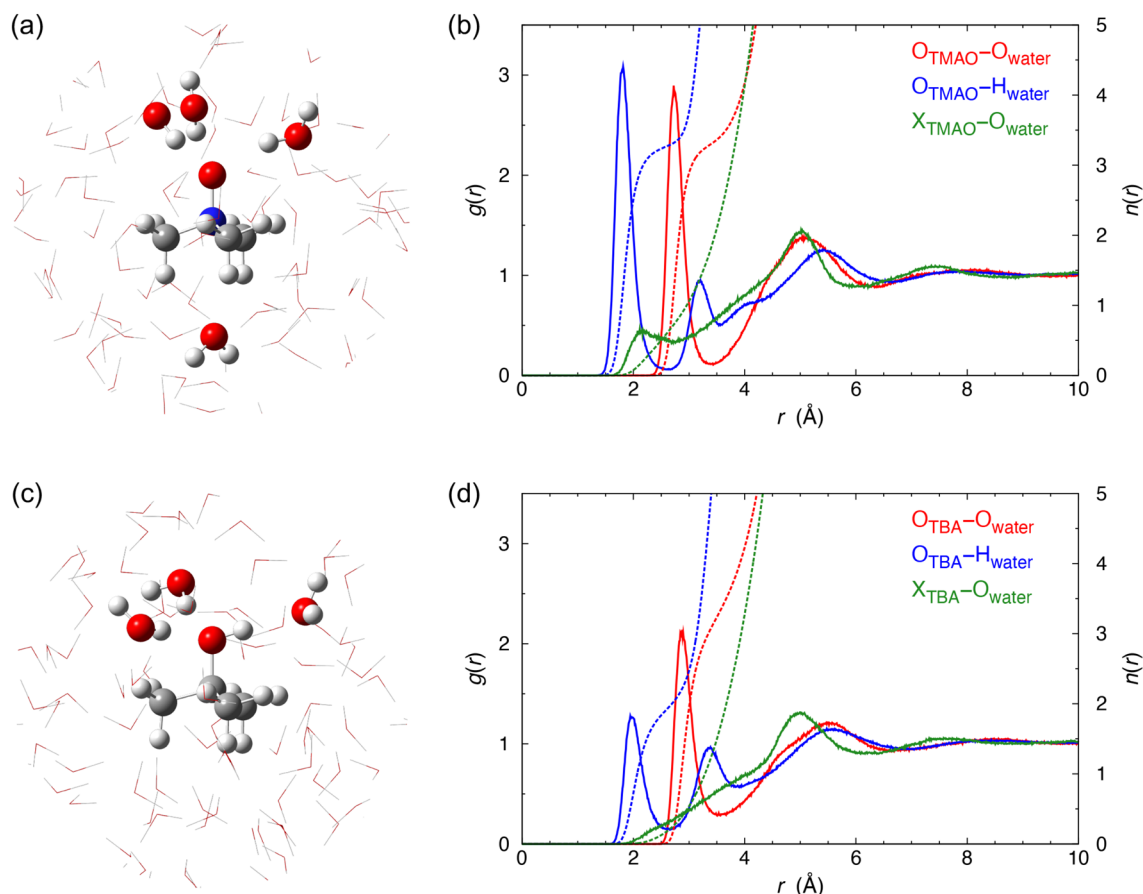
Figure 1. Solution structures simulated by EFP-MD. (**a**) Snapshot of aqueous TMAO. (**b**) Solute–solvent site RDFs, $g(r)$, and hydration numbers, $n(r)$, for aqueous TMAO. (**c**) Snapshot of aqueous TBA. (**d**) Solute–solvent site $g(r)$ and $n(r)$ for aqueous TBA. $X_{TMAO/TBA}$ was defined as the center of mass of the three axial hydrogen atoms of the CH_3- groups in TMAO/TBA.

Here, $h(t)$ is a step function defined as 1 when the distance between each solute and solvent site is smaller than the first minimum of each RDF (Table S5). Otherwise, $h(t)$ is defined as 0. The TMAO/TBA···H_2O interaction lifetimes (Table S6) were evaluated by fitting $p(t)$ to $ae^{-t/\tau_a} + be^{-t/\tau_b} (a + b = 1)$ to the data in the range $0 < t < 100$ ps (Fig. S6); the double exponential fitting was applied since it provided better results than those from the single exponential fitting.

The EFP-MD results indicated that the N^+O^- group of TMAO and the OH group of TBA captured three H_2O molecules with an average lifetime of 31.2 and 16.5 ps, respectively. The calculated lifetime for TMAO agreed with those obtained by dielectric spectroscopy (at least 50 ps at ~ 300 K)[13] and previous AIMD simulations (30–50 ps at 320 K; for D_2O solution)[19]. The lifetime near the CH_3- group of TBA could not be defined due to the lack of a hydration shell (see Fig. 1), while that near TMAO was 6.9 ps. It was confirmed that the CH_3- groups of TMAO could capture water.

EFP-MD can be utilized to investigate the time evolution of dipole moments in dilute aqueous TMAO/TBA solutions. The dipole moment of the water molecule shown in Fig. 2 is enhanced (maximally 4.20 D) when it approaches the N^+O^- group of TMAO. Similarly, when a water molecule approaches the OH group of TBA, the dipole moment is enhanced (maximally 3.78 D). The ensemble averages indicate that water molecules near the N^+O^- group of TMAO ($r < 3.5$ Å) and the corresponding OH group of TBA increased the dipole moment by an average of 3.22 D (+ 12%) and 3.01 D (+ 5%), respectively, compared to the water molecules in pure water (Table S7). The former exhibits a more significant dipole moment because TMAO has a large dipole moment of 9.39 D in an aqueous solution. In general, molecules are stabilized by polarization in aggregated systems. Surprisingly, compared to the water molecules in pure water, the water molecules near the CH_3- group of TMAO and TBA were found to have a decreased dipole moment (by −1% and −3%, respectively; Table S7). This is because the steric barrier of the CH_3- group allows only a small number of water molecules to be coordinated around the waters with decreased dipole moments. The ensemble averages of the dipole moments indicate that the influence of the solute on water converges around 4.5 Å (Fig. 3 and Table S7).

The enhancing and diminishing of polarization on the surrounding water are considered to appear as differences in the interaction energy components (E^{ES}, E^{EXREP}, E^{POL}, E^{CT}, and E^{DISP}) in the aqueous TMAO/TBA solution (Figs. 4, S7, S8, and Tables S8, S9). Therefore, the interaction energy components near the hydrophilic/hydrophobic groups are discussed.
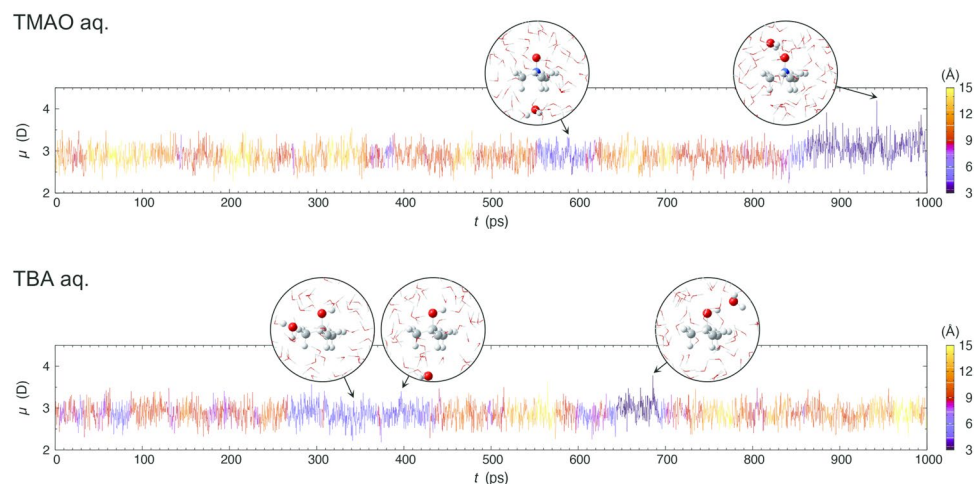
Figure 2. Temporal evolution examples of water dipole moments along 1 ns EFP-MD. The plot color represents the distances (N_{TMAO}–O_{water}/C_{TBA}–O_{water}) as indicated by the key on the right.
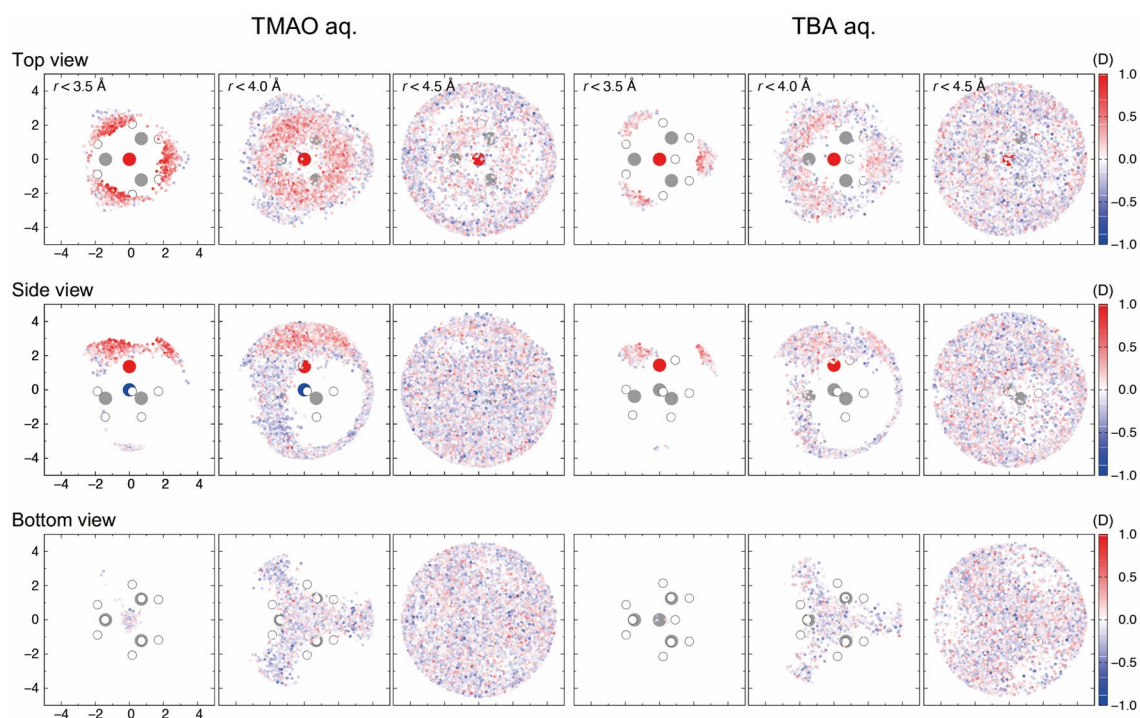
Figure 3. 1 ns water fluctuation colored by the dipole moments of H_2O molecules. The water molecules within 3.5, 4.0, and 4.5 Å from the solute are observed from the top, side, and bottom. The plot color represents the deviation from the pure water (2.87 D).

First, the solute–solvent polarization and charge-transfer interactions in the vicinity of the N^+O^- sites ($r < 3.5$ Å) in the TMAO solution were more than twice those corresponding to the OH sites in the TBA solution (Figs. 4, S7, and Table S8). The NBO analysis explains the charge-transfer interaction with a dimer model (Figs. S9, S10 and Table S10). The proton acceptor orbital of TMAO has a significant overlap integral with the H_2O orbital around the hydrophilic group and facilitates the charge-transfer (0.04 e). However, the orbital overlap between the OH group of TBA and H_2O is small; thus, the charge-transfer is small (0.01 e). Therefore, we can conclude that the factors that cause the N^+O^- group to strongly supplement water in an aqueous TMAO solution are the polarization and charge-transfer interactions derived from the large polarization of TMAO.

Next, we analyzed the interaction between the CH_3– group and the surrounding water molecules ($r < 3.5$ Å) in a TMAO/TBA solution. In this instance, the difference in the solute does not cause any difference in the charge-transfer and dispersion interactions (Figs. 4, S8, and Table S9). This can be explained by the small overlap between the proton donor orbitals of the CH_3– groups of TMAO/TBA and the molecular orbitals of water
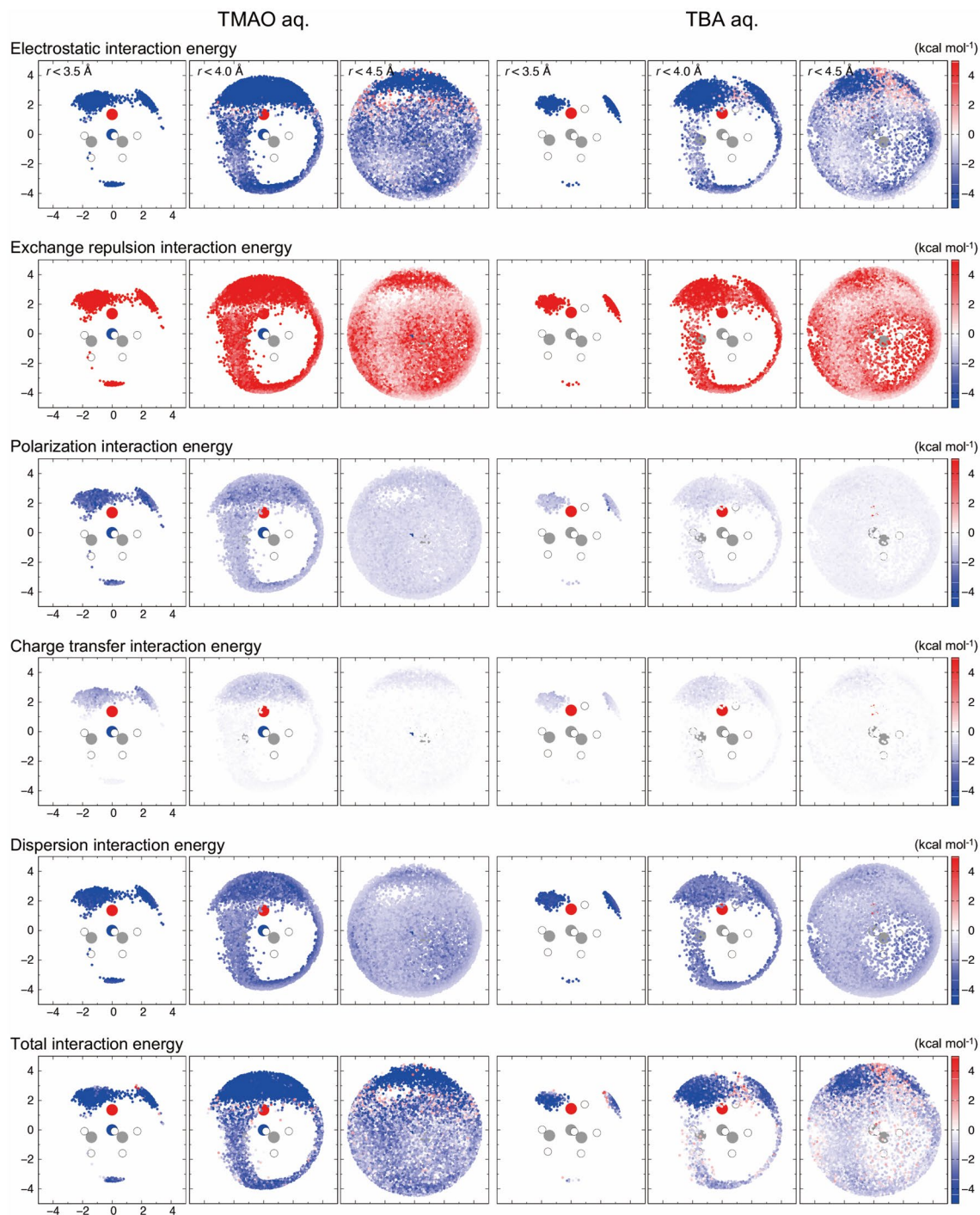
Figure 4. 1 ns water fluctuation colored by TMAO/TBA–water interactions. The water molecules within 3.5, 4.0, and 4.5 Å from the solute are observed from the side.

(Figs. S9, S10, Table S10). However, the polarization interaction energy of TMAO is more than twice that of TBA. The large dipole moment of TMAO in an aqueous solution affects even the CH_3- group. Assuming that the polarization interaction was zero, the interaction between the CH_3- group of TMAO and water would stabilize at -0.8 kcal mol^{-1} because of the contribution of the dispersion interaction, which is similar to that of TBA, and a hydrophobic interaction would be induced. In conclusion, the attractive interactions near the CH_3- group of TMAO are characterized by polarization interactions.

Conclusions

This study represents an unprecedented attempt to discuss the influence of an osmolyte TMAO and a denaturant TBA on the electronic state fluctuation of dilute aqueous solutions by analyzing the time evolution of the intermolecular interactions; these interactions can be evaluated back to their physicochemical origin only via the ab initio

EFP-MD method. The nanosecond-order EFP-MD method succeeded in reproducing the experimental results, i.e., TMAO and TBA slow the dynamics of water molecules. We analyzed the stabilizing effects of enthalpy, focusing on solute–solvent interactions. Our simulation results indicated that in dilute aqueous solutions, the dipole moment of the water molecules near the hydrophilic group of TMAO and TBA increased by an average of 12% and 5%, respectively. The dipole moment of the CH_3- group decreased by an average of −1% and −3% for TMAO and TBA, respectively. When the chemical structures of the solutes were similar, the solute–solvent interaction characteristics changed depending on the local structure and polarity of the site. TMAO allowed stable polarization and charge-transfer interactions with water molecules near the hydrophilic group, and the large solute polarization affected water molecules near the CH_3- group. However, the polarization of TBA was negligible and did not affect water molecules near the CH_3- group; the interaction was hydrophobic. The effect of small amphiphilic molecules on the change in the electronic state in aqueous solutions is significant, and it will be necessary in the future to investigate the mechanism by which osmolytes and denaturants control the stability of proteins in biological environments using ab initio simulations taking electronic fluctuation effects into account.

Data availability

Data generated or analyzed during this study are included in the main article or Supplementary information.

References

1. Yancey, P. H., Clark, M. E., Hand, S. C., Bowlus, R. D. & Somero, G. N. Living with water stress: Evolution of osmolyte systems. *Science* **217**, 1214–1222 (1982).
2. Liao, Y.-T., Manson, A. C., DeLyser, M. R., Noid, W. G. & Cremer, P. S. Trimethylamine *N*-oxide stabilizes proteins via a distinct mechanism compared with betaine and glycine. *Proc. Natl. Acad. Sci. USA* **114**, 2479–2484 (2017).
3. Bennion, B. J. & Daggett, V. Counteraction of urea-induced protein denaturation by trimethylamine *N*-oxide: A chemical chaperone at atomic resolution. *Proc. Natl. Acad. Sci. USA* **101**, 6433–6438 (2004).
4. Canchi, D. R., Jayasimha, P., Rau, D. C., Makhatadze, G. I. & Garcia, A. E. Molecular mechanism for the preferential exclusion of TMAO from protein surfaces. *J. Phys. Chem. B* **116**, 12095–12104 (2012).
5. Freda, M., Onori, G. & Santucci, A. Infrared study of the hydrophobic hydration and hydrophobic interactions in aqueous solutions of *tert*-butyl alcohol and trimethylamine-*N*-oxide. *J. Phys. Chem. B* **105**, 12714–12718 (2001).
6. Sinibaldi, R. *et al.* The role of water coordination in binary mixtures. A study of two model amphiphilic molecules in aqueous solutions by molecular dynamics and NMR. *J. Phys. Chem. B* **110**, 8885–8892 (2006).
7. Rezus, Y. L. A. & Bakker, H. J. Observation of immobilized water molecules around hydrophobic groups. *Phys. Rev. Lett.* **99**, 148301 (2007).
8. Qvist, J. & Halle, B. Thermal signature of hydrophobic hydration dynamics. *J. Am. Chem. Soc.* **130**, 10345–10353 (2008).
9. Panuszko, A., Bruździak, P., Zielkiewicz, J., Wyrzykowski, D. & Stangret, J. Effects of urea and trimethylamine-*N*-oxide on the properties of water and the secondary structure of hen egg white lysozyme. *J. Phys. Chem. B* **113**, 14797–14809 (2009).
10. Bakulin, A. A., Pshenichnikov, M. S., Bakker, H. J. & Petersen, C. Hydrophobic molecules slow down the hydrogen-bond dynamics of water. *J. Phys. Chem. A* **115**, 1821–1829 (2011).
11. Mazur, K., Heisler, I. A. & Meech, S. R. THz spectra and dynamics of aqueous solutions studied by the ultrafast optical Kerr effect. *J. Phys. Chem. B* **115**, 2563–2573 (2011).
12. Munroe, K. L., Magers, D. H. & Hammer, N. I. Raman spectroscopic signatures of noncovalent interactions between trimethylamine *N*-oxide (TMAO) and water. *J. Phys. Chem. B* **115**, 7699–7707 (2011).
13. Hunger, J., Tielrooij, K., Buchner, R., Bonn, M. & Bakker, H. J. Complex formation in aqueous trimethylamine-*N*-oxide (TMAO) solutions. *J. Phys. Chem. B* **116**, 4783–4795 (2012).
14. Ma, J., Pazos, I. M. & Gai, F. Microscopic insights into the protein-stabilizing effect of trimethylamine *N*-oxide (TMAO). *Proc. Natl. Acad. Sci. USA* **111**, 8476–8481 (2014).
15. Ganguly, P., Polák, J., van der Vegt, N. F. A., Heyda, J. & Shea, J.-E. Protein stability in TMAO and mixed urea–TMAO solutions. *J. Phys. Chem. B* **124**, 6181–6197 (2020).
16. Bandyopadhyay, D., Kamble, Y. & Choudhury, N. How different are the characteristics of aqueous solutions of *tert*-butyl alcohol and trimethylamine-*N*-oxide? A molecular dynamics simulation study. *J. Phys. Chem. B* **122**, 8220–8232 (2018).
17. Markthaler, D., Zeman, J., Baz, J., Smiatek, J. & Hansen, N. Validation of trimethylamine-*N*-oxide (TMAO) force fields based on thermophysical properties of aqueous TMAO solutions. *J. Phys. Chem. B* **121**, 10674–10688 (2017).
18. Paul, S. & Patey, G. N. Why *tert*-butyl alcohol associates in aqueous solution but trimethylamine-*N*-oxide does not. *J. Phys. Chem. B* **110**, 10514–10518 (2006).
19. Usui, K. *et al.* Ab initio liquid water dynamics in aqueous TMAO solution. *J. Phys. Chem. B* **119**, 10597–10606 (2015).
20. Imoto, S., Forbert, H. & Marx, D. Water structure and solvation of osmolytes at high hydrostatic pressure: Pure water and TMAO solutions at 10 kbar versus 1 bar. *Phys. Chem. Chem. Phys.* **17**, 24224–24237 (2015).
21. Stirnemann, G., Duboué-Dijon, E. & Laage, D. Ab initio simulations of water dynamics in aqueous TMAO solutions: Temperature and concentration effects. *J. Phys. Chem. B* **121**, 11189–11197 (2017).
22. Imoto, S., Forbert, H. & Marx, D. Aqueous TMAO solutions as seen by theoretical THz spectroscopy: Hydrophilic versus hydrophobic water. *Phys. Chem. Chem. Phys.* **20**, 6146–6158 (2018).
23. Xie, W. J. *et al.* Large hydrogen-bond mismatch between TMAO and urea promotes their hydrophobic association. *Chem* **4**, 2615–2627 (2018).
24. Sahle, C. J. *et al.* Hydration in aqueous osmolyte solutions: The case of TMAO and urea. *Phys. Chem. Chem. Phys.* **22**, 11614–11624 (2020).
25. Ghosh, D. *et al.* Noncovalent interactions in extended systems described by the effective fragment potential method: Theory and application to nucleobase oligomers. *J. Phys. Chem. A* **114**, 12739–12754 (2010).
26. Mori, H., Hirayama, N., Komeiji, Y. & Mochizuki, Y. Differences in hydration between *cis*-and *trans*-platin: Quantum insights by ab initio fragment molecular orbital-based molecular dynamics (FMO-MD). *Comput. Theor. Chem.* **986**, 30–34 (2012).
27. Matsuda, A. & Mori, H. Theoretical study on the hydration structure of divalent radium ion using fragment molecular orbital-molecular dynamics (FMO-MD) simulation. *J. Solution Chem.* **43**, 1669–1675 (2014).
28. Kuroki, N. & Mori, H. Effective fragment potential version 2-molecular dynamics (EFP2-MD) simulation for investigating solution structures of ionic liquids. *Chem. Lett.* **45**, 1009–1011 (2016).
29. Kuroki, N. & Mori, H. Applicability of effective fragment potential version 2-molecular dynamics (EFP2-MD) simulations for predicting excess properties of mixed solvents. *Chem. Phys. Lett.* **694**, 82–85 (2018).

30. Kuroki, N. & Mori, H. Applicability of effective fragment potential version 2-molecular dynamics (EFP2-MD) simulations for predicting dynamic liquid properties including the supercritical fluid phase. *J. Phys. Chem. B* **123**, 194–200 (2019).
31. Frisch, M. J. *et al. Gaussian 16, Revision C.01* (Gaussian, Inc, 2019).
32. Dunning, T. H. Jr. Gaussian basis sets for use in correlated molecular calculations. I. The atoms boron through neon and hydrogen. *J. Chem. Phys.* **90**, 1007–1023 (1989).
33. Lee, T. J. & Taylor, P. R. A diagnostic for determining the quality of single-reference electron correlation methods. *Int. J. Quant. Chem.* **36**, 199–207 (1989).
34. Schmidt, M. W. *et al.* General atomic and molecular electronic structure system. *J. Comput. Chem.* **14**, 1347–1363 (1993).
35. Su, P. & Li, H. Energy decomposition analysis of covalent bonds and intermolecular interactions. *J. Chem. Phys.* **131**, 014102 (2009).
36. Harris, K. R. & Woolf, L. A. Pressure and temperature dependence of the self diffusion coefficient of water and oxygen-18 water. *J. Chem. Soc. Faraday Trans. 1* **76**, 377–385 (1980).
37. Clark, M. E., Burnell, E. E., Chapman, N. R. & Hinke, J. A. Water in barnacle muscle. IV. Factors actors contributing to reduced self-diffusion. *Biophys. J.* **39**, 289–299 (1982).
38. Luzar, A. & Chandler, D. Hydrogen-bond kinetics in liquid water. *Nature* **379**, 55–57 (1996).

Acknowledgements

Author contributions

N.K. and H.M. conceptualized the study. T.F. developed the EFP-MD code under the supervision of H.M. Y.U. and T.F. performed the EFP-MD simulations and analyzed the results under the supervision of N.K. and H.M. N.K. visualized the results. Y.U. and N.K. wrote the original draft of the manuscript, with contributions from the other authors. N.K. and H.M. edited the manuscript. All the coauthors read and commented on the successive drafts of the manuscript.

Competing interests

The authors declare no competing interests.

Additional information

Supplementary Information The online version contains supplementary material available at https://doi.org/10.1038/s41598-022-24049-0.

Correspondence and requests for materials should be addressed to N.K. or H.M.

Reprints and permissions information is available at www.nature.com/reprints.

Publisher's note Springer Nature remains neutral with regard to jurisdictional claims in published maps and institutional affiliations.